LANGMUIR

pubs.acs.org/Langmuir Article

Creating Asymmetric Phospholipid Vesicles via Exchange With Lipid-Coated Silica Nanoparticles

Yangmingyue Liu, Elizabeth G. Kelley, Krishna C. Batchu, Lionel Porcar, and Ursula Perez-Salas*



III Metrics & More



Article Recommendations

Lipid exchange

Silica supported membrane membrane

Asymmetric Free-standing membrane membrane membrane

ABSTRACT: Recently, effort has been placed into fabricating model free-floating asymmetric lipid membranes, such as asymmetric vesicles. Here, we report on the use of lipid-coated silica nanoparticles to exchange lipids with initially symmetric vesicles to generate composition-controlled asymmetric vesicles. Our method relies on the simple and natural exchange of lipids between membranes through an aqueous medium. Using a selected temperature, time, and ratio of lipid-coated silica nanoparticles to vesicles, we produced a desired highly asymmetric leaflet composition. At this point, the silica nanoparticles were removed by centrifugation, leaving the asymmetric vesicles in solution. In the present work, the asymmetric vesicles were composed of isotopically distinct dipalmitoylphosphatidylcholine lipids. Lipid asymmetry was detected by both small-angle neutron scattering (SANS) and proton nuclear magnetic resonance (¹H NMR). The rate at which the membrane homogenizes at 75 °C was also assessed.

■ INTRODUCTION

ACCESS I

Lipids are essential components of cell membranes. In eukaryotic cells, membranes bound compartments with specialized functions requiring unique protein and lipid compositions.² The plasma membrane (PM), for example, is known to have a strict asymmetric distribution of lipids between the exoplasmic and cytoplasmic bilayer leaflets, and this structure is responsible for the physiological fate of the cells.^{2,3} The quest to understand lipid trafficking within and between membranes as it relates to lipid homeostasis and metabolism, and how this lipid organization leads to function, has led to numerous studies over the past four decades. 3d,4 Indeed, transbilayer flip-flop rates and energetics can influence interorganelle lipid transport by rearranging lipids from the inner to outer leaflets or vice versa. This rearrangement can directly affect membrane curvature and consequently vesicle budding, vesicle fission, and vesicle fusion.3d,5 Thus, there is an interplay between the rates and energetics of lipid transport that is crucial for the establishment and maintenance of an asymmetric lipid distribution across cellular membranes, which impact the strategies the cell establishes to do so.

The simplest way to study lipid flip—flop is to follow the homogenization of lipid composition in an initially asymmetric

membrane. This appeared to be straightforward to do on supported lipid bilayers, until it became clear that even very smooth surfaces create defects in the membrane, which produce an accelerated rate of leaflet mixing.⁷ To circumvent the effect of the surface, it is therefore necessary to build freefloating asymmetric membranes, such as vesicles, suitable to be measured by noninvasive, highly sensitive spatial temporal techniques like small-angle neutron scattering (SANS) and ¹H NMR. The use of cyclodextrins has proven to be a robust approach to creating asymmetric membranes in submicron-size vesicles.8 However, as the field advances, it is important to recall that until recently, the rates of the transverse movement of lipids across a lipid bilayer were reported with great dissimilarities. Therefore, when protocols are conceived, attention has to be paid to potential biases and artifacts. Finding new approaches to produce asymmetry in the

Supporting Information

Received: April 23, 2020 Revised: July 2, 2020 Published: July 6, 2020





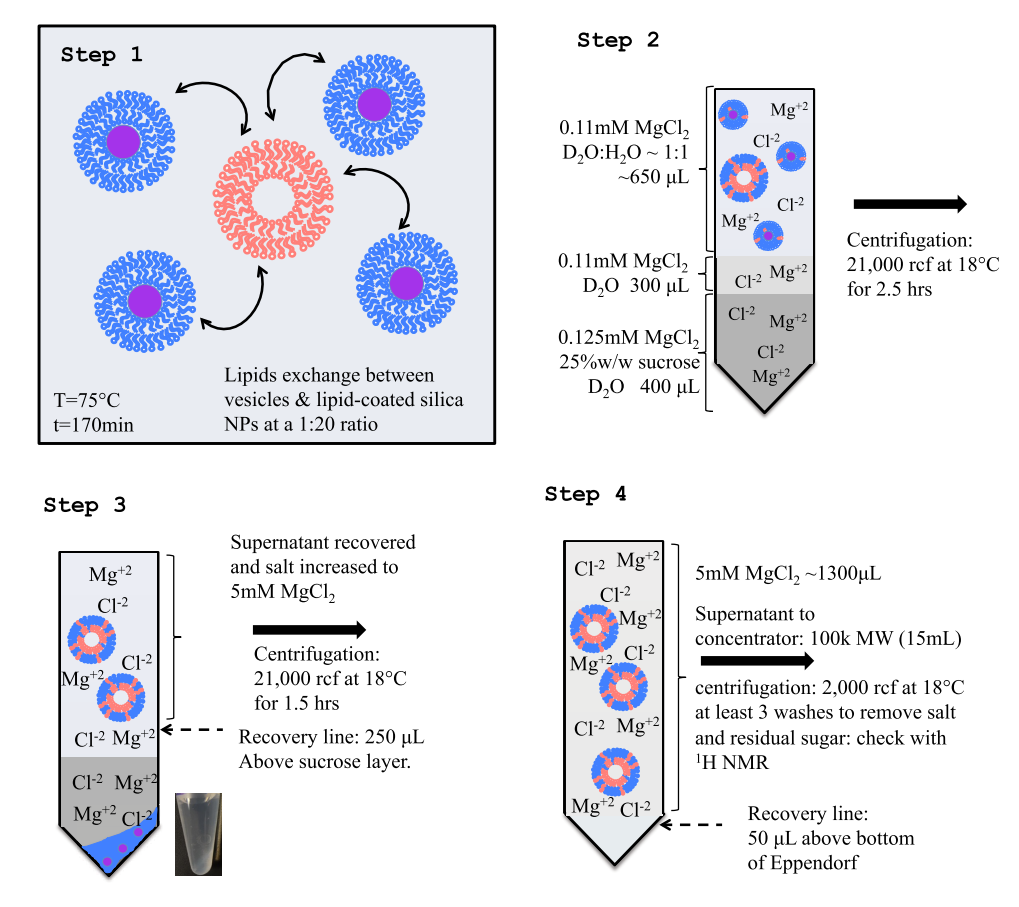


Figure 1. Illustration of asymmetric vesicle preparation, Step 1: A mixture of ≈ 50 nm vesicles (d62DPPC or d75DPPC) and hDPPC-coated 30 nm silica NPs (1:20) was annealed at 75 °C for 170 min. Step 2: Diluted in D_2O and at a 0.11 mM (M = mol/L) MgCl₂ concentration, the mixtures are loaded onto sucrose gradients and centrifuged at 21 000 rcf for 2.5 h at 18 °C. Step 3: Recovery of the supernatant well above the sucrose line. Step 4: The sample, now at 5 mM MgCl₂, is centrifuged at 21 000 rcf for 1.5 h at 18 °C and the supernatant is placed in a 15 mL, 100 000 g/mol molecular weight cutoff concentrator and washed at least three times to remove the salts and residual sugar. The last two washes are with D_2O . A check with 1H NMR will show the degree of sugar removal and if additional washes are necessary. Figure S2 in the Supporting Information shows the spectra of d75DPPC/hDPPC asymmetric vesicles having only lipid peaks and a $\approx 1\%$ H_2O peak.

membranes can only but help confirm (or not) the results and also allow for new discoveries.

Here, we present a different and novel method for preparing submicron-sized asymmetric vesicles (≈50 nm in diameter) based on the exchange of lipids between lipid-coated silica nanoparticles and vesicles through the aqueous environment. 10 The optimum annealing time, annealing temperature, and the ratio of vesicles to lipid-coated silica nanoparticles depend on the system, but these parameters ultimately determine the composition and asymmetry of the vesicle population of interest.¹¹ Once a desired lipid composition is reached, lipidcoated nanoparticles are removed by centrifugation, leaving the asymmetric vesicles in solution. These asymmetric submicron size vesicles were then characterized by high-resolution techniques (1H NMR, SANS, gas chromatography (GC), and calorimetry). We found that, for the system studied, which was predominantly the exchange between isotopically distinct dipalmitoylphosphocholine (DPPC) molecules, these vesicles can attain a high level of asymmetry in lipid composition with no residual lipid-coated silica nanoparticles contaminating the signal or potentially producing spurious and unwanted effects. In addition, the asymmetric DPPC vesicle system revealed that the rate at which the membrane homogenizes is, at least for DPPC, consistent with the results by Marquardt et al., who utilized the cyclodextrin approach to produce asymmetric

vesicles.^{7b} This suggests that although cyclodextrin is still found in their system after centrifugation, its presence is not producing any measurable effects on lipid motion within the bilayer.

MATERIALS AND METHODS

Materials. 1,2-Dipalmitoyl-sn-glycero-3-phosphocholine (hDPPC), 1,2-dipalmitoyl-d62-sn-glycero-3-phosphocholine (d62DPPC), 1,2-dipalmitoyl-d62-sn-glycero-3-phosphocholine- $1,1,2,2-d_4-N,N,N$ -trimethyl- d_9 (d75DPPC), and 1-palmitoyl-2-oleoylsn-glycero-3-phospho-(1'-rac-glycerol) (sodium salt) (POPG) were obtained as powders from Avanti Polar Lipids (Alabaster, AL) and used without further purification. LUDOX AS-40, a mass fraction of 40.8% colloidal silica solution with SiO₂ nanoparticles having a diameter of 30 nm, was purchased from Sigma-Aldrich (lot 200703) and was used as received. The LUDOX AS-40 solution's pH is 10.1 and its specific gravity is in the range between 1.295 and 1.337 g/mL. The SiO₂ beads were prepared by the water glass process and had densities of 2.2-2.6 g/cm³ (reported by the manufacturer). HPLC grade ethanol was purchased from Fisher Chemicals. Deionized water was further purified with a Millipore Simplicity UV purifier. D₂O (99.8%) and deuterated- d_6 benzene (D, 99.5%) were obtained from Cambridge Isotope Laboratories, Inc. Praseodymium(III) nitrate hexahydrate Pr(NO₃)₃·6H₂O (Pr³⁺) was purchased from Fisher Scientific and prepared as a 10 mM (M = mol/L) stock solution in D₂O. Centrifugal filter devices (Amicon Ultra-15, 100 kDa molecular weight cutoff) were purchased from EMD Millipore and washed seven times with Milli Q H₂O before use to remove trace glycerol following the protocol by Doktorova et al.⁸

Preparation of Unilamellar Lipid Vesicles. The lipids, in powder form, were used as received. Precise amounts of d62DPPC or d75DPPC and POPG were weighed out in a vial. The molar amount of POPG used was 2 mol %. Chloroform was added to the vials and stirred sufficiently to disperse all lipids. Dry lipid films on the wall of the vials were obtained by applying a constant stream of nitrogen to the chloroform solutions. The vials were then placed in a vacuum oven overnight at 70 °C to assure the complete removal of chloroform. The dried dDPPC/POPG mixtures were then redispersed in $\rm D_2O$.

We prepared unilamellar vesicles $\approx\!50$ nm in diameter via the extrusion method. This nominal size was given by the mesh size of the polycarbonate membranes used during the extrusion process. The precise size of the vesicles was determined using small-angle neutron scattering (described below) and was found to be $\approx\!50$ nm in diameter and unilamellar, as described in the Results and Discussion Section. Indeed, a few mol % of charged lipids have recently been shown to produce very stable unilamellar vesicles. 12

The extrusion process consists of the following steps. Lipid solutions are passed between two 1 mL Hamilton syringes connected to a polycarbonate membrane holder. The extruder system, consisting of the two syringes and the polycarbonate membrane holder, is placed on an extruder holder, which is kept heated by a circulating water bath set to 55 °C, which is well above the $T_{\rm m}$ of dDPPC. The lipid solution is then passed through the polycarbonate membrane 41 times with the aid of a modified New Era programmable syringe pump.

Preparation of Lipid-Coated Silica Nanoparticles. The assembly of a single bilayer coating of 30 nm diameter silica nanoparticles (NPs) was done via a solvent-exchange method, 13 as described previously. 7a In short, for this work we combined hDPPC (0.13 g) with 3 mol % of POPG (0.0045 g) dissolved in 1.25 mL of ethanol. Addition of charged lipids is necessary to keep the silica nanoparticles in suspension. 7a After the lipids are homogeneously dispersed and the ethanol solution becomes transparent at room temperature (heating to 50 °C accelerates this step), approximately 580 µL of LUDOX AS-40 silica solution, having a weight in the vicinity of 0.774 ± 0.002 g, where the uncertainty represents one standard deviation, and 680 µL of Milli Q H2O are added to the ethanol solution and vortexed vigorously for about 1 min. The vial is then placed at 50 °C until the suspension becomes somewhat clear. A second vigorous vortexing step (0.5-1 min) and another 50 °C incubation for approximately 30 min will produce a clear suspension with very little residue at the bottom of the vial. To remove all ethanol from the suspension and obtain a fully aqueous solution, the sample is dialyzed six times with warm water on a heated plate (set to 45 °C) using Spectra/Por Biotech Grade Pre-wetted Dialysis Tubing with a pore size of 100-500 Da over a span of 2-3 days (about 2.5 mL of lipid-coated silica nanoparticle solution in the dialysis bag to 0.75 mL of Milli Q H₂O bath times six changes). Some precipitation developed during the dialysis process and was removed, after the sample was recovered, using a small benchtop centrifuge at 2000 rcf (rcf = relative centrifugal force, $\times g$) for a few seconds. The volume recovered is approximately 3 mL, giving a final lipid concentration of approximately 40 mg/mL. The dialysis exchange of H₂O to D₂O could certainly be a preferred additional step that can facilitate the recovery of asymmetric lipid vesicles as described below.

Asymmetric Lipid Vesicle Preparation. The schematic for this process is shown in Figure 1. A single batch of a well-mixed solution of hDPPC + 3 mol % POPG bilayer coating of 30 nm silica nanoparticles and d62DPPC + 2 mol % POPG or d75DPPC + 2 mol % POPG of \approx 50 nm vesicles at a mass ratio of 20:1 mg was separated into several \approx 650 μ L aliquots (lipid concentration \sim 30 mg/mL) and incubated at 75 °C for 170 min (step 1). The mol % of POPG was chosen to create a stable lipid-coated nanoparticle solution using the minimal doping possible, but also POPG promoted both vesicles and lipid-coated silica nanoparticles to repel and thus avoid potential direct contact or collisions between particles. After the samples were cooled (the samples can be put in the refrigerator for fast cooling),

they were diluted in D₂O such that the volume approximately doubled. Applying a few microliters of a concentrated stock solution of MgCl₂ in D_2O (5-10 mM, M = mol/L) on the cap of the Eppendorf tube, followed by manual and fast mixing, a final salt concentration of 0.11 mM MgCl₂ was achieved. Using a small benchtop centrifuge at 2200 rcf for ≈ 1 min may show some precipitation, indicating that the lipid-coated silica nanoparticle suspension has been slightly destabilized by the salt. 1 supernatant is then layered on top of a sugar gradient in a 1.5 mL Eppendorf. The use of a sugar gradient with a relatively high salt content was to quickly destabilize the lipid-coated silica nanoparticles, favoring their speedy precipitation, and separate them from the vesicles, thus minimizing the centrifugation time or the need for ultracentrifugation. The sucrose gradient consisted of a bottom layer of 400 μ L of 25% w/w sucrose and 0.125 mM (M = mol/L) MgCl₂ in D_2O , followed by a 300 μL carefully pipetted (ie, avoiding the mixing of the layers) "buffer-zone" layer of 0.11 mM (M = mol/L) MgCl₂ in D₂O. The top layer, also carefully pipetted, was our vesicle-silica solution (\$\approx 650 \mu L). The Eppendorf tubes are then centrifuged at 21 000 rcf for at least 2.5 h at 18 °C (step 2) using an Eppenddorf 5804R benchtop centrifuge. Asymmetric vesicles, now separated from the lipid-coated nanoparticles, were obtained from the top supernatant, up to 250 μ L above the sucrose layer. For additional precaution, the supernatant's salt concentration was further increased to 5 mM (M = mol/L) MgCl₂ and centrifuged at 21 000 rcf for another 1.5 h at 18 °C (step 4). Taking all but the last 50 μ L, the samples were then placed in a 15 mL, 100 000 g/mol molecular weight cutoff centrifugal concentrator. The concentrators were prerinsed seven times with Milli Q H₂O to remove glycerol as per Doktorova et al.⁸ The concentrator tube was used to remove the salts and residual sugar with at least three washes followed by a final sample concentration step. It should be noted that a lower-molecularweight concentrator could certainly be preferred to increase the vesicle yield, as the sample is lost during the washes with the 100 000 g/mol molecular weight cutoff filter. The last two washes are done with D2O. A check with ¹H NMR will show the degree of sugar removal and if additional washes are necessary. Figure S2 in the Supporting Information shows the spectra of d75DPPC/hDPPC asymmetric vesicles having only lipid peaks, ≈1% H₂O peak, and no ethanol or sugar residue.

To check whether that the lipid-coated silica nanoparticles were removed during steps 2–4, we devised a negative control: we followed all of the steps just described before but without vesicles. Using dynamic light scattering (DLS), we confirmed that there were no particles in the solution after step 3.

Because removing lipid-coated silica nanoparticles is critical to detecting the asymmetry reliably and with DLS we could only analyze a negative control, we performed an additional SANS experiment to highlight any possible remaining nanoparticles. The experiment consisted in mixing d62DPPC vesicles with d62DPPC-coated silica nanoparticles and following the protocol through all of the steps shown in Figure 1. Figure S4, in the Supporting Information, shows the scattering signal from the d62DPPC vesicles and those recovered after exchanging with d62DPPC-coated nanoparticles. Because the scattering curve spectra overlap, we confirmed that there were no remaining d62DPPC-coated nanoparticles in the solution.

Small-Angle Neutron Scattering (SANS). SANS is a powerful technique to obtain the structure information of particles ranging from a few to hundreds of nanometers in size because the scattered intensity, I(Q), is directly related to their shape, size, and composition. A critical part in obtaining this information is to have contrast. Contrast is derived from the specific chemical and isotope-dependent scattering length densities (SLD) in the particle and the solvent. To detect compositional asymmetry across the bilayer of vesicles, the two leaflets of the membrane must display contrast. Isotopic differences come from the substitution of hydrogen with deuterium, which results in drastically different SLDs; for example, the tail SLD for hDPPC is $-0.4 \times 10^{-6} \, \text{Å}^{-2}$, while for d62DPPC (with 62 deuterium substitutions), it is $7.4 \times 10^{-6} \, \text{Å}^{-2}$. Mixtures of "d" and "h" lipids will produce varying leaflet SLDs according to the volume

fraction of each lipid type. In contrast to hydrogen and deuterium substitutions, the SLD difference between POPG and hDPPC due to their chemical compositions is insignificant, both giving essentially identical SLD values.

The SANS data were acquired on the NGB30 SANS instruments at the National Institute of Standard and Technology Center for Neutron Research (NIST-CNR), Gaithersburg, MD, and on D22 at the Institut Laue Langevin Grenoble. For the characterization of vesicles, data was taken over a broad Q-range: 0.004 Å⁻¹< Q < 0.44 $Å^{-1}$, at room temperature. Here, Q is the magnitude of the scattering vector given by $Q = 4\pi \sin(\theta/2)/\lambda$, where θ is the scattering angle and λ is the neutron wavelength. The wavelength used was 6 Å. The wavelength spread $(\Delta \lambda/\lambda)$ of 15% and 10% was used on NGB30 SANS and D22, respectively. Data were collected using a twodimensional (2D) detector and reduced using the reduction packages provided by NIST-CNR and ILL, obtaining, ultimately, circularly averaged intensity vs Q scattering curves. To have the highest possible contrast between the vesicles and the solvent and the lowest possible background, particularly in the high Q region of the spectra, we used D_2O .

¹H NMR. Proton NMR (¹H NMR) is a powerful technique to probe the structural and compositional properties of individual membrane leaflets of vesicles in solution (in D2O), particularly through the use of a shifting agent, like the paramagnetic salt Pr3+. When Pr3+ is added to a solution of unilamellar vesicles, it only has access to the outer leaflet headgroup: its choline group. As a result, the otherwise single choline peak from both the inner and outer leaflets splits into two: the inner leaflet choline, having no access to Pr³⁺, remains unshifted, while the outer leaflet choline peak is shifted due to its interaction with Pr3+. In asymmetric vesicles composed of d75DPPC and hDPPC, the ¹H NMR signal is only due to the choline group of hDPPC because in fully deuterated d75DPPC the choline hydrogens are all substituted by deuteriums and do not contribute to the ¹H NMR signal. Thus, in the presence of Pr³⁺, the relative area fractions of the shifted and unshifted choline peaks correspond to the fractional distribution of hDPPC in these vesicles. 7b,8,16

All spectra were collected on a 400 MHz Bruker DPX spectrometer and using the TopSpin 1.3 acquisition software. One-dimensional (1D) 1 H NMR experiments were acquired with 64 scans per spectrum, 10 kHz sweep width, 8192 acquisition points, and 2 s recycle delay. The pulse angle was set to 30° at a 50 kHz RF field. The spectra were processed within Topspin and converted into an XY text format for analysis with Mathematica software.

From a single asymmetric vesicle preparation, separate annealing times were studied: as prepared and annealed at 75 °C for 6 and 22 h. The volume of the samples was 0.55 mL, to which 3.9 μL was added from a 10 mM (M = mol/L) Pr³+ stock solution for a final Pr³+ concentration of 0.07 mM (M = mol/L). The vesicle concentration was ≈ 1 mg/mL. The 5 mm NMR tubes were loaded with a sealed capillary containing deuterated benzene. Data were taken at 50 °C (above the chain melting temperature of both hDPPC and d75DPPC) and the corresponding shifted and unshifted choline peaks were fitted with a sum of two Lorentzian functions to determine the inner and outer leaflet area fractions.

Gas Chromatography (GC). The lipid exchange efficiency can be fully resolved by obtaining the ratio of isotopically distinct lipids in the asymmetric vesicles using the sn-1 fatty acid methyl ester (FAME) derivatives (i.e., methyl palmitate and methyl palmitate-d31) by capillary gas chromatography as described previously. The details are included in the Supporting Information.

μ-Differential Scanning Calorimetry (DSC). μ-DSC measurements were obtained on a Setaram Micro DSC III Instrument. The sample volume was ≈320 μL, with the same corresponding volume of D_2O in the reference vessel. The vessels were introduced to the DSC at 20 °C and equilibrated for 15 min. The scan rate during heating, from 20 to 50 °C, was 1 °C/min.

RESULTS AND DISCUSSION

Asymmetric vesicles were produced using either d62DPPC \approx 50 nm vesicles or d75DPPC ≈ 50 nm vesicles mixed with hDPPC-coated silica nanoparticles, as described in detail in the Materials and Methods section. Upon mixing, lipid exchange occurs between the outer leaflet of the deuterated bilayers of the vesicles and the protiated bilayers coating the silica nanoparticles. Because in the present case, intervesicle lipid exchange is much faster than intrabilayer flip-flop due to the high ratio of the donor (lipid-coated silica nanoparticles) to acceptor (vesicles) populations, the isotope labeling scheme used here results in asymmetric vesicles that have a majority of deuterated dDPPC in the inner leaflet and protiated hDPPC in the outer leaflet. Once a "desired" asymmetry is reached in the vesicles through the length of the incubation time, the bilayercoated silica nanoparticles are easily removed by centrifugation, leaving only the asymmetric vesicles in solution. The resulting distribution of hDPPC in each leaflet of the dDPPC acceptor vesicles was quantitatively determined by isotopesensitive techniques such as SANS and ¹H NMR, in combination with GC and calorimetry. ¹H NMR was used to determine the distribution of hDPPC in hDPPC/d75DPPC vesicles because d75DPPC, having no protons, is completely invisible. Thus, the ¹H NMR signal corresponds only to the distribution of hDPPC in the vesicles. On the other hand, d62DPPC, which has a protonated headgroup, allows SANS to highlight the tail region of the lipid bilayer, which is ideal in determining the distribution of hDPPC in hDPPC/d62DPPC vesicles. GC and calorimetry provided checks on the overall composition of the vesicles.

SANS measurements of d62DPPC-only vesicles (in D_2O) and hDPPC/d62DPPC vesicles are shown in Figure 2. The

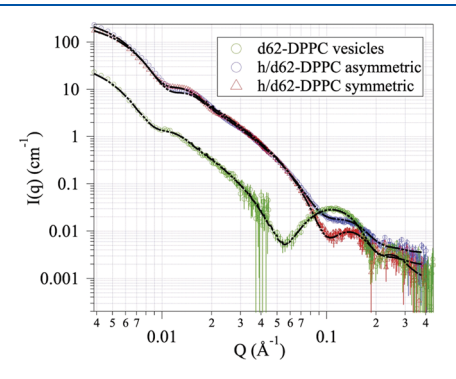


Figure 2. SANS spectra for d62DPPC vesicles (green), hDPPC/d62DPPC as-prepared asymmetric vesicles (blue), and symmetric vesicles (red) produced by annealing asymmetric vesicles at 75 $^{\circ}$ C for 22 h. The lines through the data correspond to fits whose parameters are shown in Table 2. The data were taken at room temperature. Uncertainty represents one standard deviation.

large difference in the low Q scattering between d62DPPC-only vesicles and those with hDPPC indicates that indeed hDPPC has been successfully transferred to d62DPPC vesicles from hDPPC-coated silica nanoparticles. Two curves for hDPPC/d62DPPC vesicles are presented in Figure 2, one corresponds to vesicles with an asymmetric distribution of hDPPC, while the other corresponds to the same hDPPC/d62DPPC vesicles but that have been annealed for 22 h at 75 °C. Not surprising, these two curves basically overlap at low Q indicating that the vesicles in these solutions have a similar size and size distribution, similar concentrations, and the same h-

lipid content. At high *Q*, however, the difference between these background-subtracted curves becomes evident, particularly around $Q \approx 0.1 \text{ Å}^{-1}$. In this Q-range, the uplift in the scattering of asymmetric vesicles compared to the scattering from the vesicles that have been allowed to homogenize is a clear indicator of a significant degree of asymmetry in the distribution of h-lipids across the asymmetric vesicles' membrane. The data were fit using SASview's core-multi shell vesicle form factor 17 consisting of four separate contributions: the headgroups (two) and tails (two). Simultaneous fits of the three data sets shown in Figure 2 were performed such that the following constraints were applied: (1) the thicknesses of the headgroup and tails were kept the same for all data sets, (2) the SLD of the headgroup was kept the same for all data sets, (3) the individual concentration for each data set was fixed according to the values found after the samples were lyophilized, (4) the tails' SLD of the symmetric sample (annealed for 22 h at 75 °C) was directly computed from the SLD values of the tails of the asymmetric sample, and, in that way, we conserved the lipid composition in the vesicles.

The SLDs for the individual heads and tails were unconstrained free parameters. The fit parameter tail values were assessed according to the results from gas chromatography (GC), presented in Table 1.

Table 1. GC Results^a

GC (mol %)	dDPPC	hDPPC	POPG
d75DPPC	96.2	0	3.8
h/d75DPPC	53.2	41.6	5.2
d62DPPC	97.2	0	2.8
h/d62DPPC	59.4 ± 0.2	$36. \pm 0.3$	4.6 ± 0.2

"Values are directly calculated from GC traces, as shown in Figure S1 in the Supporting Information. Uncertainty corresponds to one standard deviation from runs of two equivalent samples ("asymmetric" and "symmetric", as shown in Figure 2).

The resulting fits to the SANS data are shown as continuous curves in Figure 2, and the fit parameter values and their standard deviation are presented in Table 2. From the SANS fit parameter values, we find that the tail region of the d62DPPC-

only membranes contains some h-lipid, 2.6 ± 1.3 vol %, where the uncertainty for all values extracted from the SANS fits represents one standard deviation, which corresponds to POPG, the only h-lipid in these vesicles, as confirmed by GC, as shown in Table 1, where a 2.8% POPG corresponds to an \sim 3.0 vol % (estimating POPG to be slightly larger—1.1 times—than hDPPC¹⁸).

The GC analysis of hDPPC/d62DPPC vesicles shows that a significant amount of hDPPC was transferred from the hDPPC-coated silica nanoparticles to the initially d62DPPConly vesicles (increasing from 0 to 36.0 mol %). Furthermore, the GC analysis shows that additional POPG was transferred to the d62DPPC-only vesicles from the hDPPC-coated silica nanoparticles too (increasing from 2.8 to 4.6 mol %). However, because the SLDs of POPG and hDPPC are indistinguishable, the SANS fit parameter values can only report their combined contributions. Notwithstanding, because the fraction of hDPPC is so dominant (being ≈88 vol % of the h-lipid contribution), the behavior of the h-lipids in each leaflet mostly represents the behavior of hDPPC. Still, to avoid misinterpretations, the discussion of the SANS results and conclusions will refer to h-lipids rather than hDPPC, except where appropriate. With this in mind, the SANS tail-region fit parameter values for the as-prepared hDPPC/d62DPPC vesicles show that the outer leaflet composition is 55.3 ± 1.3 vol % h-lipids, while in the inner leaflet, it is 21.8 ± 1.3 vol %. Knowing that in these small unilamellar vesicles (SUVs), the outer leaflet has a larger volume fraction than the inner leaflet (\approx 55 vs \approx 45 vol %, respectively), this result immediately suggests that the distribution of h-lipid is highly asymmetric across leaflets. Indeed, we obtain that 75.6 \pm 2.6 mol % of the h-lipids in the vesicles reside in the outer leaflet and 24.4 ± 1.6 mol % reside in the inner leaflet. Using the volume fraction of h-lipids in the outer and inner leaflets, we also obtained that the overall h-lipid composition in the vesicles: 40.2 ± 2.1 vol %, which is, within the error, the same value that obtained in the GC analysis.

Once the hDPPC/d62DPPC vesicles were annealed for 22 h at 75 $^{\circ}$ C, the SANS tail-region fit parameter values indicated that the initially asymmetric vesicles had become symmetric. The SLD value of the tail region indicates an overall h-lipid

Table 2. Fit Parameters and Corresponding Least Square Values for the Scattering Curves Shown in Figure 2^a

SANS fit parameters	d62DPPC	h/d62DPPC	h/d62DPPC
		t = 0	t = 22 h
thickness headgroup (Å)	9.6 ± 0.1	9.6 ± 0.1	9.6 ± 0.1
thickness tail (Å)	17.1 ± 0.1	17.1 ± 0.1	17.1 ± 0.1
SLD headgroup ($\times 10^{-6} \text{ Å}^{-2}$)	2.9 ± 0.1	2.9 ± 0.1	2.9 ± 0.1
SLD inner tail ($\times 10^{-6} \text{ Å}^{-2}$)	7.1 ± 0.1	5.7 ± 0.1	4.3 ± 0.1
SLD outer tail ($\times 10^{-6} \text{ Å}^{-2}$)	7.1 ± 0.1	3.1 ± 0.1	4.3 ± 0.1
radius (Å)	285 ± 2	224 ± 2	243 ± 2
radius polydispersity	0.3	0.3	0.3
total bilayer thickness (Å)	53.3 ± 0.3	53.3 ± 0.3	53.3 ± 0.3
bilayer thickness polydispersity	0.15	0.15	0.15
h-tail vol % in inner leaflet	2.6 ± 1.3	21.8 ± 1.3	39.8 ± 1.3
h-tail vol % in outer leaflet	2.6 ± 1.3	55.3 ± 1.3	39.8 ± 1.3
mol % h in inner leaflet relative to total h	45.7 ± 2.1	24.4 ± 1.6	$45. \pm 2.1$
mol % h in outer leaflet relative to total h	54.3 ± 2.1	75.6 ± 2.6	$55. \pm 2.1$

[&]quot;Also reported are the corresponding values of the vol % of h-lipids in each leaflet derived from the fit parameter values of the tail region as well as the distribution of h-lipid between the outer and inner leaflets. Uncertainties represent the standard deviation.

composition in the vesicles of 39.8 ± 1.3 vol %, consistent, within the error, with the GC analysis.

To validate the SANS results and test the reproducibility of the technique, we employed ¹H NMR. Our interest was to capture the choline group of hDPPC in hDPPC/d75DPPC vesicles. As described in the Materials and Methods Section, d75DPPC-only vesicles do not produce any signal in the choline region because all the headgroup hydrogens in d75DPPC have been substituted by deuteriums. POPG, which is added to d75DPPC to form the vesicles, lacks the choline group, and therefore does not contribute to any signal in this region of the spectra either.

Figure 3 shows the ¹H NMR spectra from the as-prepared asymmetric hDPPC/d75DPPC vesicles (in blue symbols) as

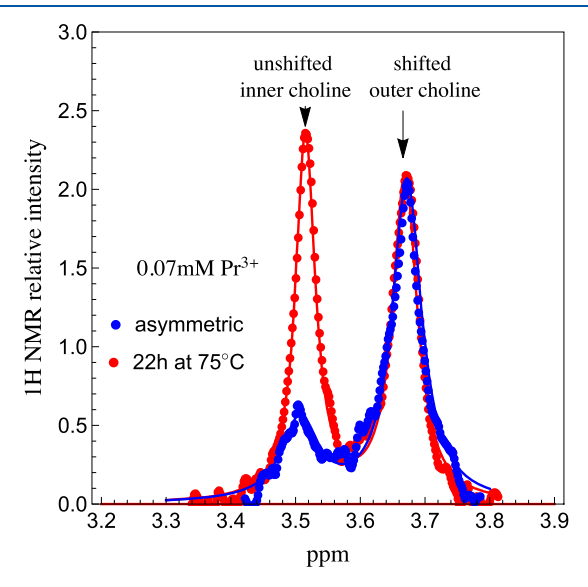


Figure 3. ¹H NMR spectra, taken at 50 °C, reveal the peaks corresponding to the choline moiety of the headgroup of hDPPC after the addition of the shifting agent Pr³⁺. The peak at 3.52 ppm corresponds to the inner leaflet choline, which has no access to Pr³⁺, while the peak at 3.67 ppm corresponds to the outer leaflet choline, which is shifted due to its exposure to Pr³⁺. Shown are asymmetric vesicles (blue) and symmetric vesicles (red) produced by annealing the asymmetric vesicles at 75 °C for 22 h. The lines through the data correspond to fits using the sum of two Lorentzians.

well as spectra from hDPPC/d75DPPC vesicles that were annealed for 22 h at 75 °C (in red symbols). Two choline peaks were detected after adding the paramagnetic salt Pr³⁺. The peak at 3.52 ppm corresponds to the inner leaflet choline, which has no access to Pr3+, while the peak at 3.67 ppm corresponds to the outer leaflet choline, which is shifted due to its exposure to Pr3+. The fact that we detect choline peaks shows that the transfer of hDPPC occurred. The GC analysis (Table 1) shows that there was a significant amount of hDPPC transferred to d75DPPC-only vesicles from the hDPPC-coated silica nanoparticles (41.6 mol % is the hDPPC concentration in the hDPPC/d75DPPC vesicles). As described in the Materials and Methods Section, from the relative area fractions of the outer and inner choline peaks, we directly obtain the distribution of hDPPC in the vesicles. Using a sum of two Lorentzians to fit these peaks (continuous lines through the data), we obtained the area for each peak and found that initially, in the as-prepared hDPPC/d75DPPC vesicles, most hDPPC is located in the outer leaflet: 76.1 ± 1.6 mol %, while

 23.9 ± 0.9 mol % is located in the inner leaflet. When these highly asymmetric vesicles are annealed for 22 h at 75 °C, the peak area fractions show that 52.7 ± 0.9 mol % of hDPPC is in the outer leaflet and 47.3 ± 0.8 mol % is in the inner leaflet, which correspond to a symmetric distribution of hDPPC in these small unilamellar vesicles.

Comparing the results on hDPPC/d75DPPC vesicles measured by ¹H NMR and the hDPPC/d62DPPC vesicles measured by SANS, we find that both systems show a large degree of asymmetry in their initial hDPPC distribution: hDPPC/d62DPPC vesicles have 75.6 \pm 2.6 mol % of the transferred h-lipids residing in the outer leaflet, while in hDPPC/d75DPPC vesicles, 76.1 ± 1.6 mol % of hDPPC resides in the outer leaflet, which means that they attained essentially the same asymmetric distribution of hDPPC within the measurement uncertainty confidence interval. From the GC analysis of hDPPC/d62DPPC and hDPPC/d75DPPC vesicles (shown in Table 1), we find that both have very similar compositions; for example, both have a slight increase in their POPG content after d62DPPC vesicles or d75DPPC vesicles were annealed with lipid-coated silica nanoparticles and both have a similar fraction of hDPPC. This result shows that the protocol is robust and reproducible.

Differential scanning calorimetry (DSC) was used to also assess the amount of hDPPC transferred to d62DPPC. Because the chain melting temperature of homogeneous mixtures of hydrogenated and tail-deuterated DPPC shifts linearly as a function of the mixture composition, 19 we were able to extract the mean fraction of hDPPC in hDPPC/ d62DPPC. Figure 4A shows chain melting heat rate peaks corresponding to ≈50 nm vesicles of d62DPPC, hDPPC, and the symmetric hDPPC/d62DPPC vesicles (after being annealed for 22 h at 75 °C). The peaks for all vesicles are broad due to not only the high curvature of these unilamellar submicron vesicles,²⁰ but also as a result of the mixing of the two isotopic species hDPPC and dDPPC.¹⁹ Using Lorentz distribution functions to fit the chain melting heat rate peaks, we found that the chain melting temperature for hDPPC (with 2 mol % POPG) was 41.15 \pm 0.01 °C, while for d62DPPC (with 2 mol % POPG), it was 37.43 ± 0.02 °C, where the uncertainty in all presented melting temperatures represents one standard deviation. These vesicles, being SUVs, have a lower $T_{\rm m}$ (~1 °C) relative to LUVs. From the peak position of symmetric hDPPC/d62DPPC vesicles (Figure 4A), we find that its chain melting temperature was 38.91 ± 0.09 °C, which meant that the molar fraction of hDPPC in the d62DPPC vesicles was 39.8 \pm 2.4 mol %, where the uncertainty represents one standard deviation and this value is within the uncertainty confidence interval of what was found by GC and SANS. Because the chain melting peak follows a linear relation with respect to the mixture of hydrogenated and deuterated DPPC, we expected to observe a broader and lower melting peak for the asymmetric vesicles. However, as shown in Figure 4B, the position, width, and height of the chain melting peaks of the symmetric and asymmetric systems coincide, suggesting that the process of chain melting is cooperative, i.e., chain melting for each leaflet occurs simultaneously, at their average composition rather than independently, and corresponding to each leaflet's very distinct composition. The chain melting curves presented in Figure 4B show, in addition, that this protocol does not have any spurious lipid contamination (i.e., lipid-coated silica or free vesicles of hDPPC).

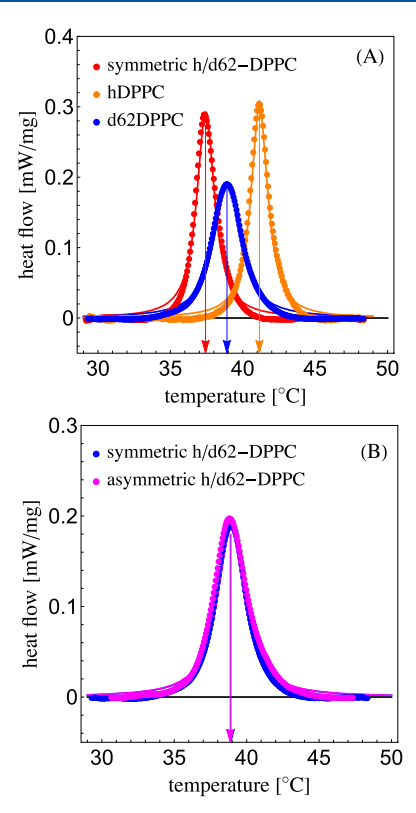


Figure 4. (A) Calorimetric traces for the chain melting of hDPPC (red, $T_{\rm m}=41.15\pm0.01~{\rm ^{\circ}C}$), d62DPPC (orange, $T_{\rm m}=37.43\pm0.02~{\rm ^{\circ}C}$), and symmetric hDPPC/d62DPPC DPPC vesicles—annealed for 22 h at 75 °C. (B) Calorimetric traces for symmetric hDPPC/d62DPPC ($T_{\rm m}=38.91\pm0.09~{\rm ^{\circ}C}$) and the asymmetric hDPPC/d62DPPC ($T_{\rm m}=38.87\pm0.04~{\rm ^{\circ}C}$) vesicles. Both symmetric and asymmetric hDPPC/d62DPPC vesicles were also measured by SANS and are shown in Figure 2. The rate of heating was 1 °C/min between 20 and 50 °C. The stated uncertainty represents one standard deviation.

Although we did not perform an in situ measurement on hDPPC/d62DPPC asymmetric vesicles to follow, in detail, the flip—flop process using SANS, we did collect ¹H NMR spectra for the case in which hDPPC/d75DPPC asymmetric vesicles, from the same batch of vesicles shown in Figure 3, were annealed for 6 h at 75 °C (see Figure S2 of the Supporting Information). The distribution of hDPPC in hDPPC/d75DPPC vesicles for unannealed vesicles and annealed for 6h and 22 h at 75 °C is shown in Table 3. This information is enough to directly compare with the previously published results on the rate of homogenization in asymmetric DPPC vesicles prepared using the cyclodextrin-mediated exchange method. ⁷⁶

Table 3. 1 H NMR Peak Area Fractions for the Outer and Inner Choline Peaks Relative to Total Choline Peak Areas as a Function of the Annealing Time at 75 $^{\circ}$ C a

¹ H NMR choline		h/d75DPPC	h/d75DPPC	h/d75DPPC
	hDPPC	t = 0	t = 6 h	t = 22 h
	mol % in inner leaflet relative to total	23.9 ± 0.9	43.6 ± 0.8	47.5 ± 0.8
	mol % in outer leaflet relative to total	76.2 ± 1.6	56.4 ± 0.8	52.7 ± 0.9

^aUncertainties represent one standard deviation.

Starting from a highly asymmetric distribution of hDPPC in the vesicles, we find that hDPPC redistributes at an estimated average flip-flop rate of $\overline{k} = 0.154 \pm 0.001 \text{ h}^{-1}$, as shown in

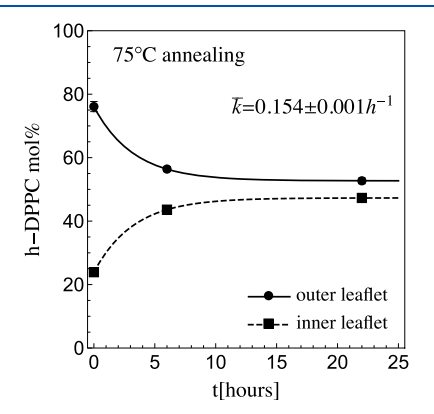


Figure 5. Distribution of hDPPC between the inner and the outer leaflets in hDPPC/d75DPPC vesicles as a function of the time taken from Table 3. The average rate of homogenization was found to be \overline{k} = 0.154 \pm 0.001 h⁻¹. Fits were done using eq 1 simultaneously. Uncertainties represent one standard deviation.

Figure 5. This value was obtained by simultaneously fitting the values presented in Table 3 using eq 1 and 2, given by

$$f_{\text{out},t} = (f_{\text{out},0} - f_{\text{out},22})e^{-2kt} + f_{\text{out},22}$$
 (1)

$$f_{\text{in},t} = (f_{\text{in},22} - f_{\text{in},0})(1 - e^{-2kt}) + f_{\text{in},0}$$
(2)

where $f_{\rm in,0}$ and $f_{\rm out,0}$ and, $f_{\rm in,22}$ and $f_{\rm out,22}$ are the respective initial and final fractions of hDPPC in the inner and outer leaflets and k is the mean flip—flop rate.

Previously Marquardt et al. studied the flip-flop rates of DPPC in 100 nm unilamellar vesicles having an asymmetric distribution of deuterated and hydrogenated headgroups using ¹H NMR.²¹ The protocol they followed to prepare asymmetric vesicles was the cyclodextrin-catalyzed lipid exchange approach.8 From the study of the flip-flop rates at different temperatures, Marquardt et al. obtained an activation energy for the flip-flop of DPPC. From this result, it is possible to extrapolate and obtain their predicted rate at 75 °C. The extrapolated flip-flop rate at 75 °C, within the error in the activation energy, is $0.115 \pm 0.004 \text{ h}^{-1}$, where the uncertainty represents one standard deviation. This value is similar to the one we found here, which suggests that, even though the system of Marquardt et al. shows the presence of some cyclodextrin according to their ¹H NMR spectra, ^{7b,16,22} it is clearly not having an effect on the flip-flop rate of DPPC. Also, the slightly higher flip-flop rate found here is consistent with a higher curvature of our vesicles.^{7a} This type of comparisons are important because, as we have argued before, the protocols can have perturbing mechanisms beyond those intended during the experimental inquiry. The use of thermally driven exchange of lipids and the ease of preparation and isolation of asymmetric vesicles, as presented here, are certainly desirable to avoid possible biases.

CONCLUSIONS

The field of the biophysics of membranes is moving forward in studying model and biological membranes that have been manipulated to create modified lipid distributions across the lipid bilayer.²³ Asymmetric membranes are now bound to be platforms for the study of many problems of biological significance, such as the role of flipases, scramblases, and transfer proteins as well as leaflet coupling,^{9,21} particularly regarding the formation of lipid rafts.^{9,16,24}

Here, we presented a novel approach to create asymmetric membranes in submicron size (≈50 nm in diameter) small unilamellar vesicles. The protocol consists of first letting a mixture of initially symmetric vesicles and silica nanoparticles coated with a single and symmetric lipid bilayer exchange lipids via a thermally driven transfer process across the aqueous environment. The composition of each leaflet of the vesicles' membrane is determined by the rate at which the outer leaflet composition changes due to the exchange with the lipid bilayer coating the silica nanoparticles and how fast the lipids flip between leaflets. Using an optimized temperature, time, and ratio of donor to acceptor populations, we achieved a highly asymmetric distribution of isotopically distinct DPPC lipids in vesicles. Once the desired asymmetric state in the vesicles was reached, the lipid-coated silica nanoparticles were easily removed by centrifugation.

This protocol offers potentially ample flexibility in asymmetric lipid compositions in submicron size (≈50 nm in diameter) vesicles. We have shown that it is possible to make a stable solution of silica nanoparticles coated with a single bilayer of dimyristoylphosphocholine (DMPC)^{7a} and now with DPPC. Certainly, there are several other lipids that are good candidates, such as other phosphocholine (PC) lipids as well as sphingomyelins, or lipid mixtures, which we plan on reporting in the near future. There are also some lipids that are clearly not good candidates to form bilayers on silica nanoparticles, for example, phosphoserine (PS) or phosphoethanolamine (PE) lipids. However, the compositional asymmetry of these lipids in vesicles can still be achieved if at least one of the other lipids of interest can form a bilayer on the silica nanoparticles. For example, we can start with PS vesicles that exchange with PC-coated silica nanoparticles or have vesicles, initially containing PE lipids (and PC), and the PC-coated silica nanoparticles would then effectively deplete the vesicles of PE. Hence, the method reported here opens potentially a new route to forming asymmetric vesicles to investigate complex and challenging dynamic flip-flop processes occurring in submicron-size vesicles.

Overall, the use of thermally driven free diffusion of lipids through an aqueous environment can be efficient in producing exchange ^{6c,10} and therefore in producing controlled asymmetry in membranes without the need to build them layer by layer, or using extraneous molecules, or having direct hemi-fusion between membranes. Because protocols can have perturbing effects beyond those intended during experimental inquiry, it is critical that we have different strategies to form asymmetric membranes to ultimately produce robust results. Indeed, herein we found that the rate at which DPPC flips and homogenizes in isotopically asymmetric membranes is similar to that found in isotopically asymmetric membranes (vesicles) prepared using the extraneous molecule cyclodextrin, suggesting that this approach is, at least for DPPC, not perturbing the system.

ASSOCIATED CONTENT

Supporting Information

The Supporting Information is available free of charge at https://pubs.acs.org/doi/10.1021/acs.langmuir.0c01188.

GC trace; ¹H NMR spectra, taken at 50 °C, for the asymmetric SUVs prepared with d75DPPC and hDPPC; choline region ¹H NMR spectra, taken at 50 °C, for asymmetric SUVs as prepared with d75DPPC and hDPPC as well as after they have been annealed for 6h and 22h at 75°C; SANS data for d62DPPC vesicles (PDF)

AUTHOR INFORMATION

Corresponding Author

Ursula Perez-Salas — Physics Department, University of Illinois at Chicago, Chicago, Illinois 60607, United States;
orcid.org/0000-0003-4675-5604; Email: ursulaps@uic.edu

Authors

Yangmingyue Liu — Physics Department, University of Illinois at Chicago, Chicago, Illinois 60607, United States

Elizabeth G. Kelley – NIST Center For Neutron Research, Gaithersburg, Maryland 20889, United States; orcid.org/ 0000-0002-6128-8517

Krishna C. Batchu – Large Scale Structure Group, Institut Laue-Langevin, Grenoble F-38042, France

Lionel Porcar – Large Scale Structure Group, Institut Laue-Langevin, Grenoble F-38042, France

Complete contact information is available at: https://pubs.acs.org/10.1021/acs.langmuir.0c01188

Author Contributions

Y.L. prepared the samples and ran the ¹H NMR and calorimetry experiments. K.C.B. ran and did the GC analysis. E.G.K. obtained the SANS data and discussed the data collection in detail. L.P. discussed the design of experiments, discussed the data collection in detail, reduced the data, programmed and ran simultaneous fitting of the SANS data, and discussed the results and manuscript in detail. U.P.-S. conceived the experiments, made the samples, analyzed ¹H NMR data and calorimetry data and SANS results, discussed all results in detail, and wrote the manuscript. All authors revised the manuscript.

Notes

The authors declare no competing financial interest.

ACKNOWLEDGMENTS

This work utilized the facilities at the National Institute for Standards and Technology, supported in part by the National Science Foundation under agreement no. DMR-0454672. Certain commercial materials are identified in this paper to foster understanding. Such identification does not imply recommendation or endorsement by the National Institute of Standards and Technology, nor does it imply that the materials or equipment identified are necessarily the best available for the purpose. The authors thank the Institute Laue Langevin for providing neutron beam time under DOI:10.5291/ILL-DATA.9-13-823. U.P.-S. additionally acknowledges the travel support from the ILL to promote scientific collaboration with L. Porcar, Y. Gerelli, and G. Fragneto. U.P.-S. gratefully acknowledges the support from the NSF CAREER award DMR-1753238.

ABBREVIATIONS

SANS, small-angle neutron scattering; TR-SANS, timeresolved SANS; ¹H NMR, proton nuclear magnetic resonance; NPs, nanoparticles; DPPC, dipalmitoylphosphocholine; hDPPC, hydrogenated DPPC; d62DPPC, 62 deuterium substitutions in DPPC; d75DPPC, 75 deuterium substitutions in DPPC; DMPC, dimyristoylphosphocholine; PC, phosphocholine; PS, phosphoserine; PE, phosphoethanolamine; d, deuterated; h, hydrogenated

REFERENCES

- (1) Yeagle, P. L. The Membrane of Cells; Academic Press, Inc.: New York, 1993.
- (2) van Meer, G.; Voelker, D. R.; Feigenson, G. W. Membrane lipids: where they are and how they behave. *Nat. Rev. Mol. Cell Biol.* **2008**, *9*, 112–124.
- (3) (a) Bretscher, M. S. Asymmetrical lipid bilayer structure for biological membranes. *Nature, New Biol.* **1972**, 236, 11–12. (b) Opdenkamp, J. A. F. Lipid Asymmetry in Membranes. *Annu. Rev. Biochem.* **1979**, 48, 47–71. (c) Skowronska-Krawczyk, D.; Budin, I. Aging membranes: Unexplored functions for lipids in the lifespan of the central nervous system. *Exp. Gerontol.* **2020**, *131*, No. 110817. (d) Mochel, F. Lipids and synaptic functions. *J. Inherited Metab. Dis.* **2018**, *41*, 1117–1122.
- (4) (a) Holthuis, J. C.; Levine, T. P. Lipid traffic: floppy drives and a superhighway. *Nat. Rev. Mol. Cell Biol.* **2005**, *6*, 209–220. (b) Nicolson, G. L. The Fluid-Mosaic Model of Membrane Structure: still relevant to understanding the structure, function and dynamics of biological membranes after more than 40 years. *Biochim. Biophys. Acta, Biomembr.* **2014**, *1838*, 1451–1466.
- (5) (a) Sprong, H.; van der Sluijs, P.; van Meer, G. How proteins move lipids and lipids move proteins. *Nat. Rev. Mol. Cell Biol.* **2001**, *2*, 504–513. (b) Lev, S. Lipid homoeostasis and Golgi secretory function. *Biochem. Soc. Trans.* **2006**, *34*, 363–366.
- (6) (a) Liu, J.; Conboy, J. C. 1,2-diacyl-phosphatidylcholine flip-flop measured directly by sum-frequency vibrational spectroscopy. *Biophys. J.* 2005, 89, 2522–2532. (b) Gerelli, Y.; Porcar, L.; Fragneto, G. Lipid Rearrangement in DSPC/DMPC Bilayers: A Neutron Reflectometry Study. *Langmuir* 2012, 28, 15922–15928. (c) Gerelli, Y.; Porcar, L.; Lombardi, L.; Fragneto, G. Lipid Exchange and Flip-Flop in Solid Supported Bilayers. *Langmuir* 2013, 29, 12762–12769.
- (7) (a) Wah, B.; Breidigan, J. M.; Adams, J.; Horbal, P.; Garg, S.; Porcar, L.; Perez-Salas, U. Reconciling differences between lipid transfer in free-standing and solid supported membranes: a time resolved small angle neutron scattering study. *Langmuir* 2017, 33, 3384–3394. (b) Marquardt, D.; Heberle, F. A.; Miti, T.; Eicher, B.; London, E.; Katsaras, J.; Pabst, G. 1H NMR Shows Slow Phospholipid Flip-Flop in Gel and Fluid Bilayers. *Langmuir* 2017, 33, 3731–3741.
- (8) Doktorova, M.; Heberle, F. A.; Eicher, B.; Standaert, R. F.; Katsaras, J.; London, E.; Pabst, G.; Marquardt, D. Preparation of asymmetric phospholipid vesicles for use as cell membrane models. *Nat. Protoc.* **2018**, *13*, 2086–2101.
- (9) Enoki, T. A.; Feigenson, G. W. Asymmetric Bilayers by Hemifusion: Method and Leaflet Behaviors. *Biophys. J.* **2019**, *117*, 1037–1050.
- (10) Pownall, H. J.; Bick, D. L.; Massey, J. B. Spontaneous phospholipid transfer: development of a quantitative model. *Biochemistry* **1991**, *30*, 5696–5700.
- (11) (a) Breidigan, J. M.; Krzyzanowski, N.; Liu, Y.; Porcar, L.; Perez-Salas, U. The membrane environment influence on cholesterol transfer. *J. Lipid Res.* **2017**, *58*, 2255–2263. (b) Nakano, M.; Fukuda, M.; Kudo, T.; Matsuzaki, N.; Azuma, T.; Sekine, K.; Endo, H.; Handa, T. Flip-flop of phospholipids in vesicles: kinetic analysis with timeresolved small-angle neutron scattering. *J. Phys. Chem. B* **2009**, *113*, 6745–6748.

- (12) Scott, H. L.; Skinkle, A.; Kelley, E. G.; Waxham, M. N.; Levental, I.; Heberle, F. A. On the Mechanism of Bilayer Separation by Extrusion, or Why Your LUVs Are Not Really Unilamellar. *Biophys. J.* **2019**, *117*, 1381–1386.
- (13) Hohner, A. O.; David, M. P.; Radler, J. O. Controlled solvent-exchange deposition of phospholipid membranes onto solid surfaces. *Biointerphases* **2010**, *5*, 1–8.
- (14) Metin, C. O.; Lake, L. W.; Miranda, C. R.; Nguyen, Q. P. Stability of Aqueous Silica Nanoparticle Dispersions under Subsurface Conditions. *J. Nanopart. Res.* **2011**, *13*, 839–850.
- (15) Pencer, J.; Mills, T.; Anghel, V.; Krueger, S.; Epand, R. M.; Katsaras, J. Detection of submicron-sized raft-like domains in membranes by small-angle neutron scattering. *Eur. Phys. J. E: Soft Matter* **2005**, *18*, 447–458.
- (16) Heberle, F. A.; Marquardt, D.; Doktorova, M.; Geier, B.; Standaert, R. F.; Heftberger, P.; Kollmitzer, B.; Nickels, J. D.; Dick, R. A.; Feigenson, G. W.; Katsaras, J.; London, E.; Pabst, G. Subnanometer Structure of an Asymmetric Model Membrane: Interleaflet Coupling Influences Domain Properties. *Langmuir* 2016, 32, 5195–5200.
- (17) SasView is a Small Angle Scattering Analysis Software Package originally developed as part of the NSF DANSE project under the name SansView and now managed by an international collaboration. https://http://www.sasview.org.
- (18) (a) Kučerka, N.; Nieh, M. P.; Katsaras, J. Fluid phase lipid areas and bilayer thicknesses of commonly used phosphatidylcholines as a function of temperature. *Biochim. Biophys. Acta* **2011**, 1808, 2761–2771. (b) Nagle, J. F.; Cognet, P.; Dupuy, F. G.; Tristram-Nagle, S. Structure of gel phase DPPC determined by X-ray diffraction. *Chem. Phys. Lipids* **2019**, 218, 168–177.
- (19) Katsaras, J.; Epand, R. F.; Epand, R. M. Absence of chiral domains in mixtures of dipalmitoylphosphatidylcholine molecules of opposite chirality. *Phys. Rev. E* **1997**, *S5*, 3751–3753.
- (20) (a) Lichtenberg, D.; Freire, E.; Schmidt, C. F.; Barenholz, Y.; Felgner, P. L.; Thompson, T. E. Effect of surface curvature on stability, thermodynamic behavior, and osmotic activity of dipalmitoylphosphatidylcholine single lamellar vesicles. *Biochemistry* 1981, 20, 3462–3467. (b) Huang, C. Studies on phosphatidylcholine vesicles. Formation and physical characteristics. *Biochemistry* 1969, 8, 344–352. (c) Lichtenberg, D.; Biltonen, R. L. The use of differential scanning calorimetry as a tool to characterize liposome preparations. *Chem. Phys. Lipids* 1993, 64, 129–142.
- (21) Eicher, B.; Marquardt, D.; Heberle, F. A.; Letofsky-Papst, I.; Rechberger, G. N.; Appavou, M. S.; Katsaras, J.; Pabst, G. Intrinsic Curvature-Mediated Transbilayer Coupling in Asymmetric Lipid Vesicles. *Biophys. J.* **2018**, *114*, 146–157.
- (22) Bauer, M.; Charitat, T.; Fajolles, C.; Fragneto, G.; Daillant, J. Insertion properties of cholesteryl cyclodextrins in phospholipid membranes: a molecular study. *Soft Matter* **2012**, *8*, 942–953.
- (23) London, E. Membrane Structure-Function Insights from Asymmetric Lipid Vesicles. *Acc. Chem. Res.* **2019**, *52*, 2382–2391.
- (24) Weiner, M. D.; Feigenson, G. W. Molecular Dynamics Simulations Reveal Leaflet Coupling in Compositionally Asymmetric Phase-Separated Lipid Membranes. *J. Phys. Chem. B* **2019**, *123*, 3968–3975.